

# Prediction of Novel $\text{BaMnO}_{3-y}$ ( $0 < y < 0.1$ ) Perovskite Related Phases

J. M. González-Calbet,<sup>\*,†,1</sup> M. Parras,<sup>\*</sup> J. Alonso,<sup>\*,†</sup> and M. Vallet-Regí,<sup>†,‡</sup>

<sup>\*</sup>Dpto. Química Inorgánica, Facultad de Químicas, Universidad Complutense, 28040 Madrid, Spain; <sup>†</sup>Instituto Magnetismo Aplicado (RENFE-UCM), Apdo. 155, 28230 Las Rozas, Madrid, Spain; and <sup>‡</sup>Dpto. de Química Inorgánica y Bioinorgánica, Facultad de Farmacia, Universidad Complutense, 28040 Madrid, Spain

Received December 10, 1993; in revised form January 26, 1994; accepted February 28, 1994

IN HONOR OF C. N. R. RAO ON HIS 60TH BIRTHDAY

An electron diffraction and microscopy study of the  $\text{BaMnO}_{3-y}$  system indicates that for  $0.1 < y < 0.25$  several types crystallize showing hexagonal symmetry, rhombohedral types being obtained for  $0 < y < 0.1$ . On the basis that oxygen deficiency is accommodated by the introduction of  $\text{BaO}_{2.5}$  cubic layers in the hexagonal close packing of  $\text{BaMnO}_3$ , the existence of different types can be predicted, taking into account that the anionic composition can be deduced from the expression  $y = 0.5c/(c + h)$ , where  $c$  and  $h$  refers to the number of cubic and hexagonal layers per unit cell, respectively. Electron microscopy proves the existence of new rhombohedral types (21R, 27R, 33R) along the  $0 < y < 0.1$  range. © 1994 Academic Press, Inc.

## 1. INTRODUCTION

Among the extensive contributions to solid state chemistry by professor Rao, particular attention has been devoted to compositional variations in perovskite-related materials (1).

$\text{AMO}_3$  related perovskites can be described on the basis of close packed  $\text{AO}_3$  layers with  $M$  cations in a fraction of octahedral sites. For a fcc oxygen packing,  $\text{MO}_6$  octahedra share corners, only three layers being necessary to describe the resulting cubic cell according to the stacking sequence ...ccc... For a hexagonal close packing,  $\text{MO}_6$  octahedra share faces, only two layers being necessary to describe the resulting  $\text{BaNiO}_3$  2H hexagonal cell according to the sequence ...hhh...

In a series of papers, Rao and co-workers (2–6) have shown that defect ordering in  $\text{AMO}_{3-x}$  perovskite-related oxides involves a conservative mechanism in the sense that the vacancies are assimilated into the structure, resulting in large supercells of the basic perovskite structure, the type of superstructure formed depending on the identity of the  $M$  cation. For instance, an interesting series of oxides prepared by the topotactic reduction

of  $\text{Ca}_2\text{Fe}_{2-x}\text{Mn}_x\text{O}_{6-y}$  is  $\text{Ca}_2\text{Fe}_{2-x}\text{Mn}_x\text{O}_5$  where three different coordination polyhedra of the transition metal coexist (7).

Nowadays, it is well established that compositional variations in  $\text{AMO}_{3-y}$  related perovskites lead to different coordination polyhedra as a function of the stability of cations occupying  $A$  and  $M$  sites. As a consequence, several ordered phases have been obtained, less attention being devoted to anionic deficient perovskites showing hexagonal packing, the nonstoichiometry being accommodated in these systems by adjusting the relative proportion of cubic and hexagonal stacking of the  $\text{AO}_{3-y}$  layers. Electron microscopy provides direct verifications of the stacking arrangement of the  $\text{AO}_3$  layers in  $\text{AMO}_3$  polytypes (8).

For instance, several phases have been described in the  $\text{BaCoO}_{3-y}$  ( $0 \leq y \leq 1$ ) system (9, 10), where Co atoms are in both octahedral and tetrahedral sites.

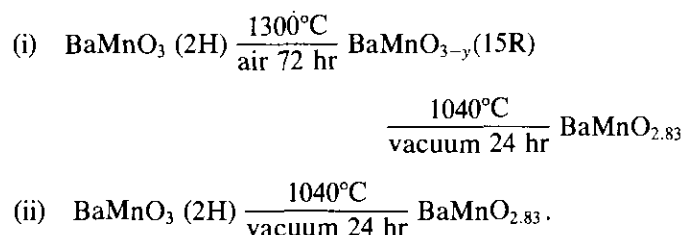
For Mn atoms occupying  $M$  sites, nonstoichiometry is accommodated in a different way. A powder X-ray diffraction study of  $\text{CaMnO}_{2.50}$  performed by Poppelmeier *et al.* (12) reveals an ordering of the oxygen vacancies not seen before in the perovskite-related structures and an unusual square pyramidal coordination for the  $\text{Mn}^{3+}$  cations formed as a consequence of the Jahn–Teller effect. Thus, in the  $\text{CaMnO}_{3-y}$  ( $0 \leq y \leq 0.5$ ) system (cubic close packing), ordered structures based on interconnected  $\text{MnO}_6$  octahedra and  $\text{MnO}_5$  square pyramids have been revealed by electron diffraction and high resolution electron microscopy (12). Such a coordination is also observed for  $\text{BaMnO}_{3-y}$  and  $\text{SrMnO}_{3-y}$  systems where, in contrast, the  $\text{AO}_x$  layers are hexagonal packed. Although both systems have been widely studied by Negas and Roth (13, 14), recent microstructural studies by means of electron diffraction and microscopy have clarified some of the information given by X-ray diffraction. Thus, according to Shibahara (15), nonstoichiometry in  $\text{SrMnO}_{3-y}$  is accommodated by the formation of planar defects as observed by means of high resolution electron microscopy (HREM).

<sup>1</sup> To whom all correspondence should be addressed.

## 2. THE BaMnO<sub>3-y</sub> SYSTEM: HOW MANY POLYTYPES CAN EXIST?

Negas and Roth (13) have shown by X-ray diffraction that BaMnO<sub>3</sub> is isostructural with BaNiO<sub>3</sub> (2H), a decreasing of the oxygen content leading to the formation of 15R, 8H, 6H, 10H, and 4H BaMnO<sub>3-y</sub> phases. In a series of previous papers (16, 17) we have reported that the oxygen deficiency in the reduction process of 2H BaMnO<sub>3</sub> hexagonal type leads to the introduction of BaO<sub>2.5</sub> cubic layers and then to the modification of the initial hexagonal close packing. If this is true, an ideal anionic composition should correspond to every hexagonal type as shown in Table 1.

As can be observed, the 6H structural type shows the BaMnO<sub>2.83</sub> composition. Such a stoichiometry can be obtained in two different ways:



Although chemical composition and powder X-ray diffraction patterns are coincident in both cases, the microstructural study indicates that only an ordered material is obtained by using the second synthetical route (16). Stacking faults observed in the 6H material obtained by the first route seems to be a consequence of the high concentration of stacking faults appearing in the intermediate 15R sample (see Fig. 2 of Ref. (16)). According to this, compositional variations in BaMnO<sub>3-y</sub> can be accommodated either by disordered intergrowths of the different hexagonal types or by formation of ordered materials. Thus, in order to obtain a BaMnO<sub>3-y</sub> ordered material, two conditions seem to be necessary: to start from a well ordered material and to reduce it to the an-

TABLE 1  
Stacking Sequence and Anionic Composition for the BaMnO<sub>3-y</sub> Structural Types

Type	Stacking sequence	Composition
2H	...hhh...	BaMnO <sub>3</sub>
15R	...(chhhh) <sub>3</sub> ...	BaMnO <sub>2.90</sub>
8H	...(chhh) <sub>2</sub> ...	BaMnO <sub>2.875</sub>
6H	...chchhhc...	BaMnO <sub>2.83</sub>
10H	...(chchh) <sub>2</sub> ...	BaMnO <sub>2.80</sub>
4H	...ch...	BaMnO <sub>2.75</sub>

ionic composition corresponding to a structural type. Thus, although Negas and Roth have proposed several routes by which to synthesize BaMnO<sub>3-y</sub> deficient perovskites, we have fixed the starting material (BaMnO<sub>3</sub> (2H)) in order to obtain ordered phases.

On the basis of the abundant information given by Negas and Roth (13), it seems that four different phases can be stabilized in the 0.1 ≤ y ≤ 0.2 compositional range (15R, 8H, 6H, and 10H), while only BaMnO<sub>3</sub> (2H) and BaMnO<sub>2.90</sub> (15R) can be isolated along 0 ≤ y ≤ 0.1.

Considering that the chemical composition of a cubic layer is BaO<sub>2.5</sub> and that corresponding to a hexagonal one is BaO<sub>3</sub>, it is possible to propose the existence of all the structural types which correspond to the anionic composition following the expression: y = 0.5c/(c + h), c and h being the number of cubic and hexagonal layers per unit cell, respectively. These compositions imply an integer number of both hexagonal and cubic layers per unit cell.

The number of types so far described in the 0 ≤ y ≤ 0.1 composition range is very small. Effectively, in this range the following structural types have been isolated:

- BaMnO<sub>3</sub> (2H): stacking sequence ...hh...
- BaMnO<sub>2.90</sub> (15R): stacking sequence ...(chhhh)<sub>3</sub>...

By varying the relationship between c and h layers, intermediate compositions should be obtained between these two structural types. Since each composition is related to a different structural type, we have studied the resulting structural types according to the symmetry of stacked closest-packed layers (18) following the Zhdanov notation.

From BaMnO<sub>2.90</sub>, ...chhhh..., the smallest possible increasing of the anionic composition should lead to a stacking sequence ...chhhhh..., c/(c + h) = 1/6. The corresponding anionic deficiency is y = 1/12. This relationship corresponds to a hexagonal cell with a double period of the stacking sequence. But keeping the relationship of c and h layers, there exist two possible stacking sequences with even period, and basic partitions:

—|21111|11112|, which corresponds to a 12H-type with the ...chchhhhhhh... stacking sequence with *P6m2* space group (Fig. 1a).

—|11(2)11|11(2)11|, which corresponds to a 12H-type with the ...(chhhhh)<sub>2</sub>... stacking sequence with *P6<sub>3</sub>mmc* space group (Fig. 1b).

For c/(c + h) = 1/7, y = 1/14, the only possible stacking sequence corresponds to an odd period with rhombohedral symmetry:

—(2)11(1)11, which corresponds to the (chhhhhh)<sub>3</sub> stacking sequence (per hexagonal unit cell) with *R3m* space group (Fig. 2a), characteristic of a 21R-type (R stands for a rhombohedral symmetry).

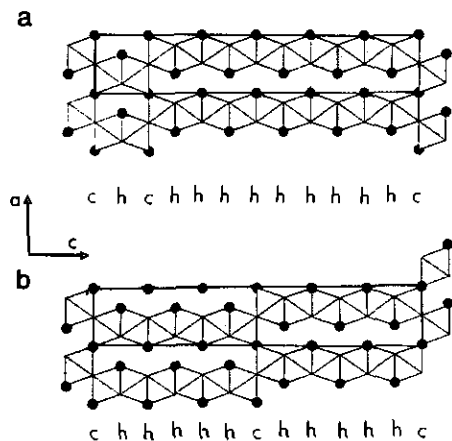


FIG. 1. Structural model projection corresponding to two 12H-polytypes: (a) Stacking sequence ...chchhhhhhhhh...; (b) Stacking sequence ...(chhhhh)<sub>2</sub>...

For  $c$  ( $c + h$ ) =  $1/8$ ,  $y = 1/16$ . As in the previous hexagonal cell ( $y = 1/12$ ) two stacking sequences are possible:

— $[2111111|1111112]$ , which corresponds to a 16H-type with stacking sequence ...chchhhhhhhhhhhhh..., with  $P6m2$  space group (Fig. 3a).

— $[111(2)111|111(2)111]$ , which corresponds to another 16H-polytype with ...(chhhhhhh)<sub>2</sub>... stacking sequence, and  $P6_3mmc$  space group (Fig. 3b).

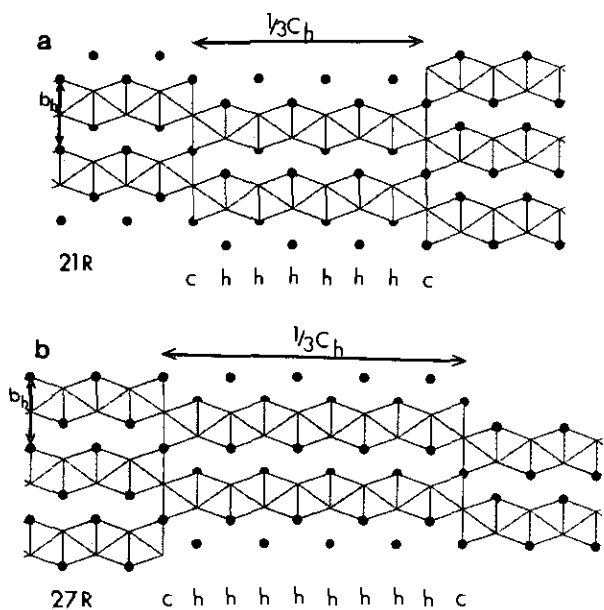


FIG. 2. Structural model projection corresponding to (a) 21R structural type; (b) 27R structural type.

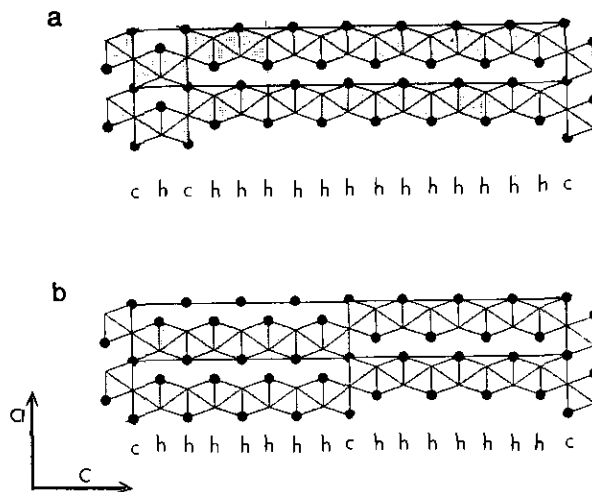


FIG. 3. Structural model projection corresponding to two 16H-polytypes: (a) Stacking sequence ...chchhhhhhhhhhhhhhh...; (b) Stacking sequence ...(chhhhhhh)<sub>2</sub>...

For  $c/h + c = 1/9$ ,  $y = 1/18$ , there exists only one possible stacking sequence:

— $(2)111(1)111$ , which corresponds to a 27R-type, with ...(chhhhhhhhh)<sub>3</sub>... stacking sequence (per hexagonal unit cell) and  $R3m$  space group (Fig. 2b).

For  $c/c + h = 1/10$ ,  $y = 1/20$ , two possibilities arise:

— $[211111111|111111112]$ , which corresponds to a 20H-type with the ...chchhhhhhhhhhhhhhhhhhh... stacking sequence with  $P6m2$  space group (Fig. 4a).

— $[1111(2)1111|1111(2)1111]$ , which corresponds to another polytype of the 20H-type with stacking sequence ...(chhhhhhhhh)<sub>2</sub>... and  $P6_3mmc$  space group (Fig. 4b).

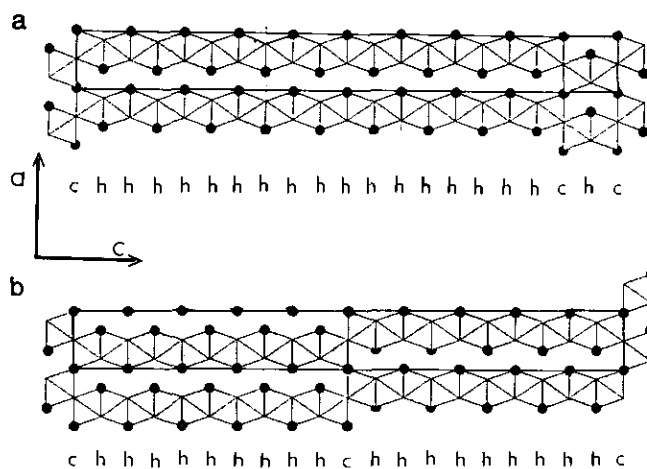


FIG. 4. Structural model projection corresponding to two 20H-polytypes: (a) Stacking sequence ...chchhhhhhhhhhhhhhhhhhh...; (b) Stacking sequence ...(chhhhhhhhh)<sub>2</sub>...

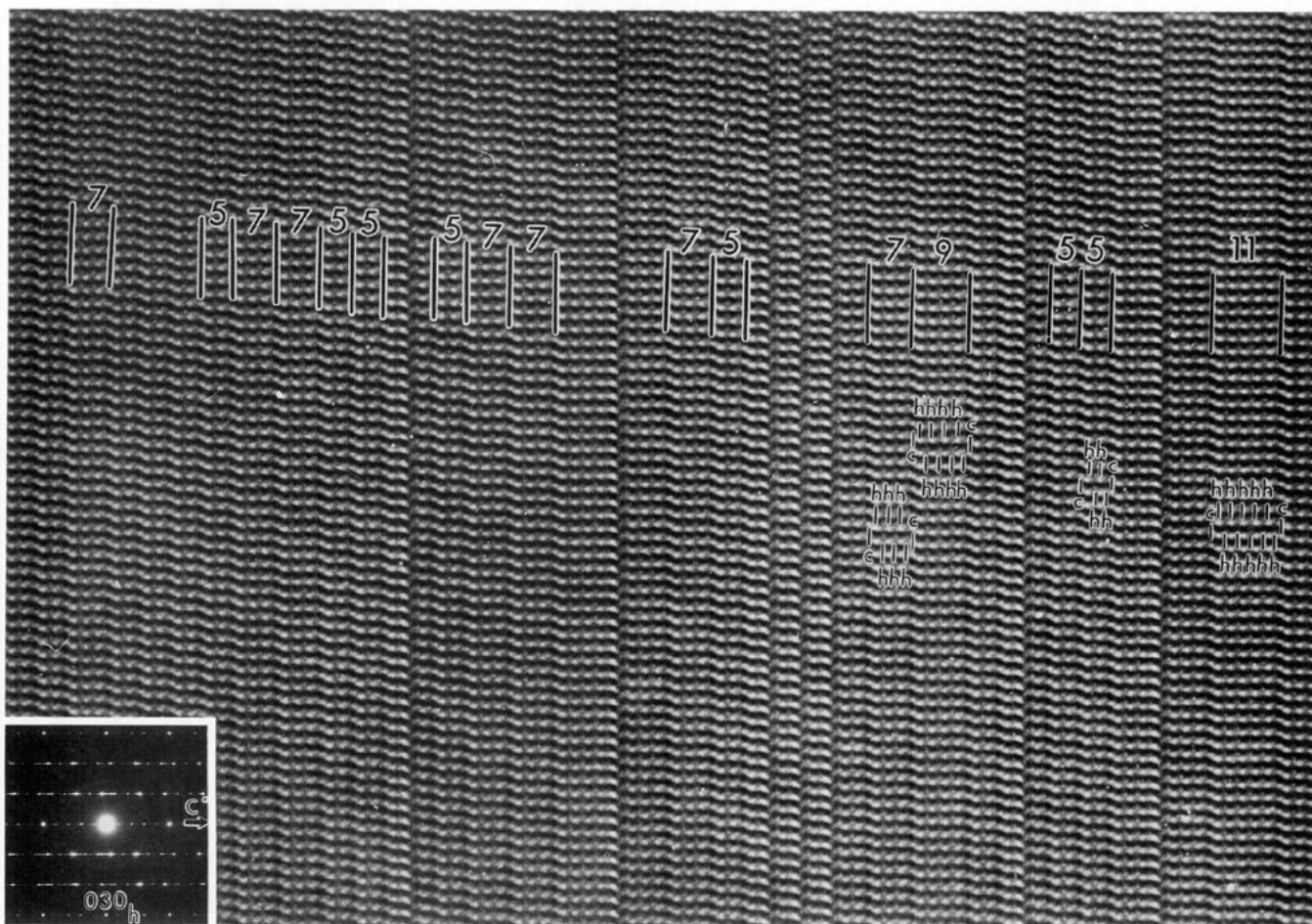


FIG. 5. HREM image along the [100] corresponding to  $\text{BaMnO}_{2.92}$ . Disordered intergrowths of 5, 7, 9, and 11 layers are seen. Corresponding electron diffraction pattern is seen at the inset.

Obviously, as the  $y$  value approaches zero, the probability of obtaining an ordered state decreases.

### 3. EVIDENCE FOR NEW TYPES ALONG THE $0 < y < 0.1$ RANGE

In order to see if these structural types can exist we have prepared a sample in the  $0 < y < 0.1$  compositional range. The thermogravimetric characterization indicates that the composition for such a sample is  $\text{BaMnO}_{2.92}$ .

The study by electron diffraction and microscopy clearly shows that this sample is highly disordered. Figure 5 shows a high resolution micrograph along the [100] zone axis. Streaking is apparent in the electron diffraction pattern shown at the inset. Most of the crystals show a similar situation, a disordered intergrowth between two structural types being observed. One of them shows the stacking sequence ...chhhh..., i.e.,  $1/3$  (15R). The other

one, as depicted in the micrograph, shows the sequence ...chhhhhh... corresponding to  $1/3$  (21R), which confirms the existence of a new type with the  $\text{BaMnO}_{2.928}$  composition.

Although the majority phases appearing in these crystals are  $\text{BaMnO}_{2.90}$  (15R) and  $\text{BaMnO}_{2.928}$  (21R), isolated lamellae corresponding to different stacking sequences are also observed. One of them, as depicted in the image, shows the stacking sequence ...chhhhhhhh..., which should correspond to  $1/3$  of the previously mentioned 27R structural type. Another set of fringes corresponds to a stacking sequence ...chhhhhhhhhh... which should correspond to  $1/3$  of a 33R structural type. We have not previously described such a type since the possibility of isolating ordered types for a value of  $y = 0.045$  remains very small. Such a structural model is depicted in Fig. 6, the Zhdanov notation being (2)1111(1)1111.

On the basis of this information, one might think that these new structural types along the  $0 < y < 0.1$  range

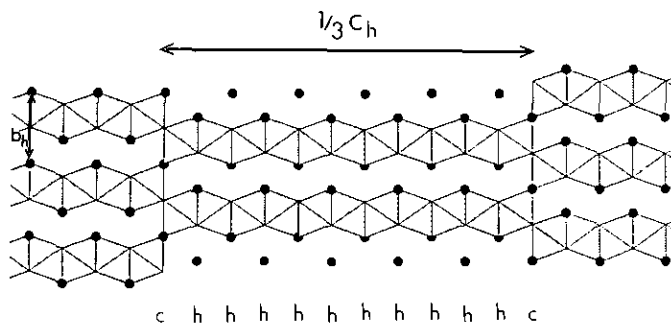


FIG. 6. Structural model projection corresponding to the 33R.

can only exist as extended defects constituted by small fractions of a given structural type intergrown on the matrix of the previously described 15R type, which seems to be the most stable along this range. However, some experimental facts indicate that it should be possible to isolate some of these phases. Effectively, Fig. 7a shows the electron micrograph of a minority kind of crystals appearing in the sample, characterized as  $\text{BaMnO}_{2.92}$ . The distance between planes is 4.9 nm, corresponding to the stacking sequence  $(\text{chhhhhh})_3$ . The corresponding electron diffraction pattern along the  $[100]_h$  zone axis

(Fig. 7b) agrees with the structural type showing rhombohedral symmetry. This  $(\text{chhhhhh})_3$  stacking sequence is repeated along all the crystal, only one stacking fault appearing, showing nine layers, which presumably corresponds to 1/3 of the 27R structural type.

It should be considered that the average composition for this sample is  $\text{BaMnO}_{2.92}$ , which is very close to the theoretical composition corresponding to the structural types more frequently appearing in this sample, i.e.,  $\text{BaMnO}_{2.90}$  (15R) and  $\text{BaMnO}_{2.928}$  (21R). The chemical compositions for the less abundant 27R and 33R types, which also show rhombohedral symmetry, is  $\text{BaMnO}_{2.944}$  and  $\text{BaMnO}_{2.954}$ , respectively. In order to isolate such phases, we will try in the future to prepare more oxidized samples with accurate control of the oxygen stoichiometry.

It is also worth mentioning that all the observed structural types in Fig. 5 show rhombohedral symmetry. This probably means that the intergrowth between different structural types is easier when they show the same symmetry. In fact, for  $y > 0.1$  all the intergrown phases up to now described show hexagonal symmetry (17), indicating that probably two different domains exist in the  $\text{BaMnO}_{3-y}$  system from the point of view of the symmetry, the threshold being  $y = 0.1$ .

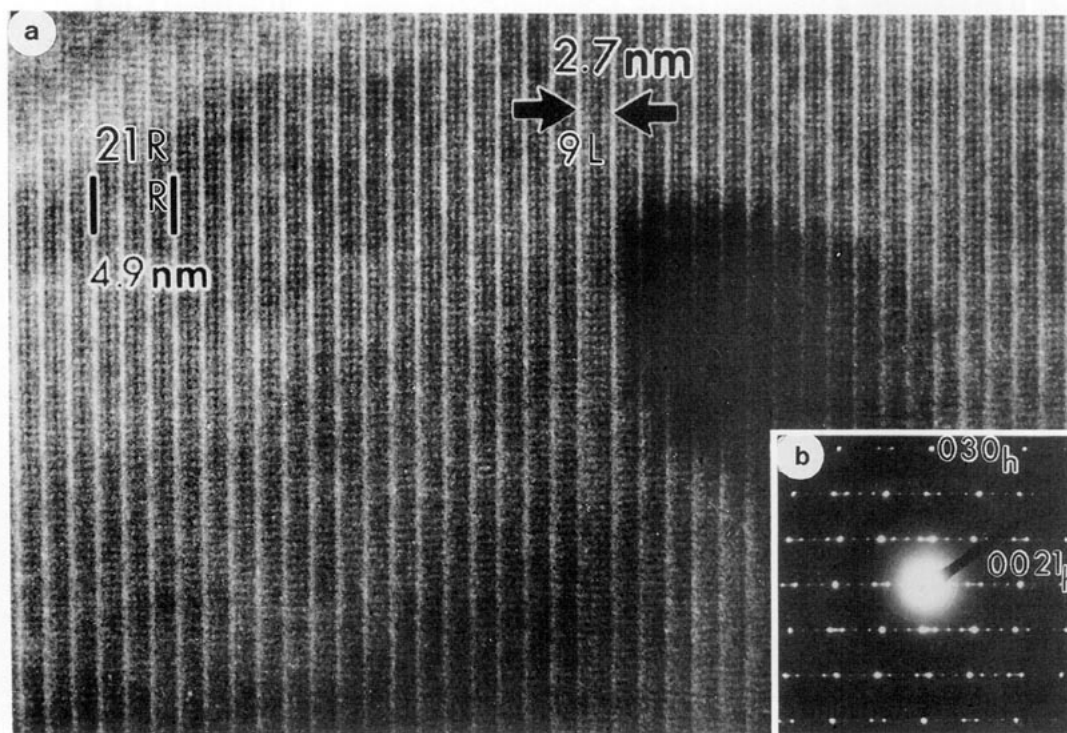


FIG. 7. Electron micrograph of a 15R crystal showing a stacking fault constituted by nine layers. (b) Corresponding electron diffraction pattern along  $[100]_h$ .

## ACKNOWLEDGMENTS

We acknowledge the financial support of CICYT (Spain) through Research Projects MAT 91-0331 and MAT 93-0207. We are also grateful to Mr. A García and Mr. E. Baldonado for valuable technical assistance.

## REFERENCES

1. C. N. Rao and J. Gopalakrishnan, "New Directions in Solid State Chemistry," Cambridge Univ. Press, Cambridge, 1989.
2. C. N. R. Rao, J. Gopalakrishnan, and K. Vidyasagar, *Indian J. Chem. Sect. A*, **23**, 265 (1984).
3. K. Vidyasagar, J. Gopalakrishnan, and C. N. R. Rao, *Inorg. Chem.* **23**, 1206 (1989).
4. K. Vidyasagar, J. Gopalakrishnan, and C. N. R. Rao, *J. Solid State Chem.* **58**, 29 (1985).
5. K. Vidyasagar, A. Reller, J. Gopalakrishnan, and C. N. R. Rao, *J. Chem. Soc. Chem. Commun.*, 7 (1985).
6. C. N. R. Rao, K. Vidyasagar, J. Gopalakrishnan, A. K. Ganguli, A. Ramanan, and L. Ganapathi, *J. Mater. Res.* **1**, 280 (1986).
7. K. Vidyasagar, L. Ganapathi, J. Gopalakrishnan, and C. N. R. Rao, *J. Chem. Soc. Chem. Commun.*, 449 (1986).
8. P. L. Gai and C. N. R. Rao, *Pramana* **55**, 274 (1975).
9. M. Zanne, A. Courtois, and C. Gleitzer, *Bull. Soc. Chim. Fr.* **12**, 4470 (1972).
10. A. J. Jacobson and J. L. Hutchison, *J. Solid State Chem.* **35**, 334 (1980).
11. M. Parras, M. Vallet-Regí, J. M. González-Calbet, and J. C. Grenier, *J. Solid State Chem.* **83**, 121 (1989).
12. K. R. Poppelmeier, M. E. Leonowicz, and J. M. Longo, *J. Solid State Chem.* **44**, 89 (1982); A. Reller, J. M. Thomas, D. A. Jefferson and M. K. Uppal, *Proc. R. Soc. London Ser. A* **394**, 223 (1984).
13. T. Negas and R. S. Roth, *J. Solid State Chem.* **3**, 323 (1971).
14. T. Negas and R. S. Roth, *J. Solid State Chem.* **1**, 409 (1970).
15. H. Shibahara, *J. Mater. Res.* **6**(3), 565 (1991).
16. M. Parras, J. M. González-Calbet, J. M. Alonso, and M. Vallet-Regí, *Solid State Ionics* **63**, 614 (1993).
17. J. M. González-Calbet, M. Parras, J. M. Alonso, and M. Vallet-Regí, *J. Solid State Chem.* **169**, 99 (1993).
18. "International Tables for X-ray Crystallography, Vol. II, p. 342. Kynoch Press, Birmingham (1959).